Dentomaxillofacial Radiology (2019) 48, 20190205

birpublications.org/dmfr

REVIEW ARTICLE

The maxillary sinus: physiology, development and imaging anatomy

[1,2,3]Andrew Whyte and [4,5]Rudolf Boeddinghaus

[1]Associate Professor, University of Western Australia, Nedlands, Western Australia, Australia; [2]Head, Neck and Maxillofacial Radiologist, Perth Radiological Clinic, Subiaco, Western Australia, Australia; [3]Associate Professor, University of Melbourne, Carlton, Victoria, Australia; [4]Radiologist, Perth Radiological Clinic, Subiaco, Western Australia, Australia; [5]Senior Lecturer, University of Western Australia, Nedlands, Western Australia, Australia

Objectives: The maxillary sinus is of paramount importance for otolaryngologists, rhinologists, oral and maxillofacial surgeons, head and neck and dental and maxillofacial radiologists. A comprehensive review article concerning the physiology, development and imaging anatomy was undertaken.
Methods: Relevant literature pertaining to the physiology of the sinonasal cavity, development of the paranasal sinuses and imaging anatomy of the maxilla and maxillary sinus from 2000 to 2019 was reviewed. Emphasis was placed on literature from the last 5 years.
Results: Extensive recent research using imaging has provided new insights into the development of the maxillary sinus, the other paranasal sinuses and the midface. The fundamental physiological concept of mucociliary clearance and its role in sinus health is emphasized. The paranasal sinuses are an integral part of a common mucosal organ formed by the upper and lower airway.
An in-depth understanding of the soft-tissue and neurovascular relationships of the maxillary sinus to the deep fascial spaces and branches of the trigeminal nerve and external carotid artery respectively is required to evaluate and report imaging involving the maxillary sinus.
Sinusitis of rhinogenic, rather than odontogenic origin, originates from nasal inflammation followed by anterior ethmoid disease and secondary obstruction of the ostiomeatal unit. The role of anatomical variants that predispose to this pattern of disease is discussed in detail with illustrative examples.
The maxillary sinus is intimately related to the roots of the posterior maxillary teeth; the high frequency of mucosal disease and sinusitis of odontogenic aetiology is now well recognized. In addition, an understanding of the anatomy of the alveolar process, morphology of the alveolar recess of the maxillary sinus and neurovascular supply are essential both for deliberate surgical intervention of the sinus and complications related to oral surgical procedures.
Conclusions: An understanding of the fundamental principles of the development, physiology, anatomy and relationships of the maxillary sinus as depicted by multi-modality imaging is essential for radiologists reporting imaging involving the paranasal sinuses and midface.
Dentomaxillofacial Radiology (2019) **48**, 20190205. doi: 10.1259/dmfr.20190205

Cite this article as: Whyte A, Boeddinghaus R. The maxillary sinus: physiology, development and imaging anatomy. *Dentomaxillofac Radiol* 2019; **48**: 20190205.

Keywords: Maxillary Sinus; Dentition – Anatomy; Physiology; Diagnostic Imaging

Introduction

There are four pairs of paranasal sinuses: the maxillary, ethmoid, frontal and sphenoid. They are air-filled, mucosa-lined spaces within the maxillofacial region and skull centred on and communicating with the nasal cavity.

The nose and paranasal sinuses form a functional unit as well as being an integral part of the respiratory tract

Correspondence to: Prof Andrew Whyte, E-mail: andywhyte7@bigpond.com
Received 23 May 2019; revised 27 July 2019; accepted 31 July 2019

with the tracheobronchial tree and lungs. Specialised epithelium filters, warms and humidifies inspired air in preparation for optimal exchange of oxygen and carbon dioxide in the lungs. Shared homeostatic and immune systems throughout the upper and lower respiratory tract form the basis of the relatively recent concept of theunified airway.[1] Disease and treatment in the upper respiratory tract affects the lower respiratory tract and vice versa, the strong link between asthma and chronic rhinosinusitis being the prime example.

The maxillary sinuses were first illustrated and described by Leonardo da Vinci in 1489 and later documented by the English anatomist Nathaniel Highmore in 1651. The maxillary sinus, or antrum of Highmore, lies within the body of the maxillary bone and is the largest and first to develop of the paranasal sinuses. The alveolar process of the maxilla supports the dentition and forms the inferior boundary of the sinus.

It is no longer acceptable to regard the maxillary sinus as having a functional division into an inferior half supporting the dentoalveolar process that is the focus of the dental specialities and a superior half which includes the sinus ostium and is the province of the rhinologist.

Furthermore, the anterior paranasal sinuses (*i.e.* the maxillary, anterior ethmoid and frontal sinuses) all drain into the ostiomeatal unit. The anterior ethmoid, not the maxillary, sinus is considered the key anterior sinus in affecting the common drainage pathway of the anterior sinus group according to the basic principles of mucociliary clearance and endoscopic sinus surgery.[2]

There is extensive evidence in the recent literature that dental sepsis commonly results in reactive mucosal thickening in the inferior aspect of the maxillary sinus. An odontogenic cause for maxillary sinusitis, and indeed sinusitis involving the anterior paranasal sinuses, is commoner than previously thought and increasing in incidence.[3] Opacification of the maxillary sinus and sinusitis involving a unilateral anterior sinus group have a dental aetiology in 75% and 25–40% of cases, respectively.

Understanding the role of the maxillary sinus in health and disease requires an in-depth knowledge of the physiology of the upper respiratory tract and of the development and the clinical and imaging anatomy of the maxillary sinus, especially its relationship to the dentition, nose and the ethmoid and frontal sinuses.

Methods

Recent articles published over the last 5 years, in the anatomical, dental, rhinological and imaging literature form the basis for this review of the physiology, development and imaging anatomy of the maxillary sinus.

Physiology: frequently referenced articles in the rhinological literature covering the role of mucociliary clearance in maintaining sinus health and the physiological basis of sinus surgery were reviewed. The more recent concept of the unified airway: a common mucosal organ including the upper and lower respiratory tract was referenced from the original review articles.

Development: there have been several articles in the recent peer-reviewed anatomical, paediatric and rhinological literature covering growth of the maxillary sinus (or paranasal sinuses in general) using cross-sectional imaging to evaluate normal development. The results are summarized as key points in the relevant section.

Abnormal development was summarized using the data both from landmark articles since the year 2000 and more recent references in the imaging, rhinological and paediatric literature.

Imaging anatomy: review articles in the radiological and rhinological literature emphasise the anatomy of the anterior sinus group: the anterior ethmoid, maxillary and frontal sinuses which drain into the ostiomeatal unit. The importance of anatomical variants in predisposing to blockage of this drainage channel or influencing endoscopic surgery are described and illustrated.

Extensive dental and maxillofacial literature and selected rhinological and imaging review articles conclude that an odontogenic cause for maxillary sinus mucosal disease and sinusitis is relatively common. The intimate relationship of the posterior maxillary teeth to the sinus and the morphology of the alveolus and alveolar recess are discussed in detail. The major review articles in the anatomical, imaging, dental and maxillofacial literature covering the osseous, neurovascular and regional soft-tissue anatomy were reviewed to provide a thorough overview with specific reference to sinus lift procedures for ridge augmentation.

Radiological experience: the authors have personal experience in reporting approximately 60,000 CT and MRI scans of the paranasal sinuses and 30,000 multidetector CT (MDCT) and cone beam CT (CBCT) scans covering the maxilla and the maxillary sinus.

For the last 17 years, rhinological cases with significant pathology or other notable findings have been discussed at a weekly joint clinicoradiological meeting in the setting of a major teaching hospital. Pathological correlation was available for all cases undergoing biopsy and surgery.

Close co-operation is also maintained with dental specialists, especially referring oral and maxillofacial surgeons.

Physiology

The nose and sinuses are lined by a pseudostratified columnar ciliated (*i.e.* respiratory) epithelium with numerous goblet cells supported by a vascular lamina propria containing serous and mucous glands and numerous thin-walled venules. Together, the epithelium and the lamina propria constitute the mucosa. Mucosa lining the nose and paranasal sinuses is bound to the underlying periosteum, and this mucoperiosteum is commonly referred to as the Schneiderian membrane.

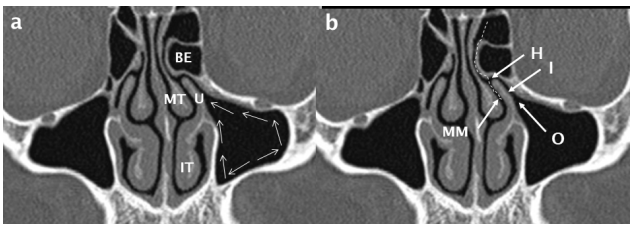

Figure 1 *The ostiomeatal unit/ complex.* Cilia propel mucus (white arrows in a) towards the sinus ostium (O); it then passes via the infundibulum (I) to the hiatus semilunaris (H) and into the middle meatus (MM). The path of drainage of mucus from the frontal sinus via the frontal recess is shown by the white dashed line in b. The anatomical boundaries of the OMU/ C include the uncinate process (U), middle turbinate (MT), inferior turbinate (IT) and the most prominent anterior ethmoid air cell: bulla ethmoidalis (BE).

Mucociliary clearance is a primary defence mechanism of the respiratory tract to protect against inhaled pollutants, allergens and pathogens.[4–6] The functional components of the mucociliary apparatus include the cilia and a protective mucous layer which is secreted by goblet cells in the epithelium and mucous glands in the lamina propria. Mucus acts like flypaper, trapping airborne particles inspired through the nose. The mucus is in two layers; a thin and watery sol layer which bathes the cilia allowing them to move easily and the superficial, thick and sticky gel layer responsible for trapping the inspired particles. Cilia act in a co-ordinated fashion to move the gel layer and trapped particles (at a rate of about 6 mm per minute) towards the sinus ostium and from there to the nose and posteriorly to the nasopharynx before being swallowed. The health of the nose and paranasal sinuses is primarily dependent on effective mucociliary clearance. Chronic rhinosinusitis leads to secondary cilial dysfunction, abnormal mucus and impaired mucociliary function.[4,7]

In the anterior sinuses (frontal, anterior ethmoid and maxillary), the mucociliary pathway always leads towards the ostiomeatal unit (OMU) or complex (Figure 1). Blockage of the OMU results in anterior sinus disease.

The combination of a large surface area provided by the nasal cavity and convolutions of the turbinates, the secreted mucus and a profuse blood supply in the lamina propria allows the nose to heat and humidify inspired air. The nose can turn dry, cold air into moist, warm air in under a second and this process of air conditioning is essential for the function and health of the lower respiratory tract (larynx, trachea, bronchi, bronchioles and alveoli).

The unified airway is a term that has been used over the last two decades that recognizes the common functions, homeostasis and immune system of the upper and lower respiratory tract. This mucosal organ includes the nose, paranasal sinuses, nasopharynx, larynx, trachea, bronchi and bronchioles.[1] Given that they have fundamentally the same epithelial lining, it is not surprising that the upper and lower airway share a common response to inhaled allergens, infective agents and other irritants. Large, long-term studies have demonstrated that subjects with allergic rhinitis or chronic rhinosinusitis are 3–4 times more likely to have or subsequently develop asthma than the general population. All are chronic inflammatory diseases with common types of inflammatory cells and mediators. Successful treatment of disease in one subsite of the respiratory tract has a beneficial effect throughout theunified airway.[8]

Additional theoretical functions of the paranasal sinuses are to minimize bone mass of the skull while providing contouring, improve the resonance of the voice and to act as a crumple zone in severe midface trauma acting in conjunction with the multiple, thin interconnecting bones supporting and surrounding the sinonasal cavity.

Normal development

The maxillary sinus (MS) is the largest paranasal sinus and the first to develop. Development commences at 17 weeks *in utero*. At birth, it is a rudimentary aerated or fluid-filled slit orientated longest in the anteroposterior dimension with a volume of 60–80 mm^3, situated inferomedial to the orbit.[9] Partial or complete opacification of the maxillary sinus in the first few years of life is normal.[10]

Growth of the MS is proportional to growth of the facial bones.[9,11] Both occur in phases with the first phase occurring during the first 3 years of life: the sinus extending lateral to the infraorbital canal by the end of this phase (Figure 2). The second phase of growth occurs during years 6–12 with lateral extension to the zygomatic recess of the maxilla and inferior extension to the level of the hard palate by 9 years of age. Subsequent sinus expansion during the third phase comes from pneumatization of the maxillary alveolus as the permanent molar and premolar teeth erupt displacing the floor of the sinus 4–5 mm below the floor of the nasal cavity.[10,12]

Development of the MS has been evaluated over the last 20 years by analysis of axial two-dimensional CT, volumetric analysis of three-dimensional scans produced by MDCT) and CBCT, as well as MRI.[9–19] Whilst there are some conflicting data, the findings can be summarized as follows:

(1) The height of the MS increases continuously up to the age of 18 years. In contrast, the width and length (anteroposterior dimension) of the MS reaches adult proportions by the age of 12 years.[13]
(2) The most rapid increase in size of the MS occurs from 0 to 4 years with a gradual increase in size from 4 to 8 years.[9]
(3) A gender difference in MS size develops after the age of 8 years with a plateau in females and a slow increase in size in males up to the age of 18 years.[9]
(4) The development of the MS continues until the third decade in males and the second decade in females.[9]

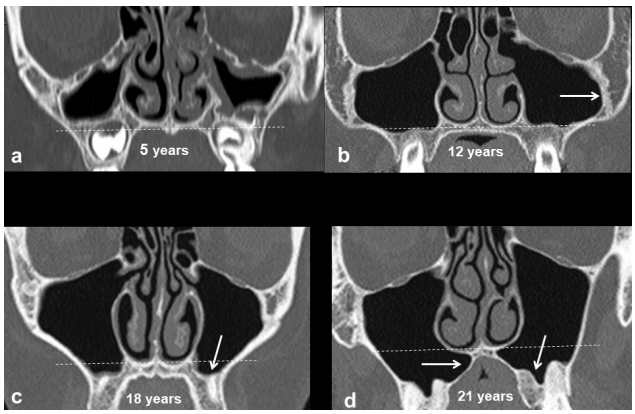

Figure 2 *Development of the maxillary sinuses.* Up to the age of 12 years, growth of the maxillary sinus is predominantly in a lateral direction towards the zygoma creating the zygomatic recess (white arrow in b) and inferiorly to the level of the hard palate. Thereafter, the sinus expands inferiorly below the level of the nasal floor (white arrows in c, d).

(5) The mean volume of the fully developed MS is larger in males than females; in most studies the difference is not significant.[9,13]
(6) Mean volumes of the MS vary according to ethnicity and tend to be larger in Japanese and Korean subjects.[9,12]
(7) Despite inferior expansion of the maxillary sinus that follows loss of a posterior maxillary tooth, especially the first molar, most studies have shown both no change in sinus volume with dentition status (presence or absence of premolars or molars) and a decrease in volume with advancing age.[12]
(8) Measurements of the adult MS vary significantly between different studies; the range of dimensions is 38–45 mm in length, 25–35 mm in width and 36–45 mm in height. The average MS volume from multiple studies is 150 mm^3 with a range of 100–250 mm^3.[15]

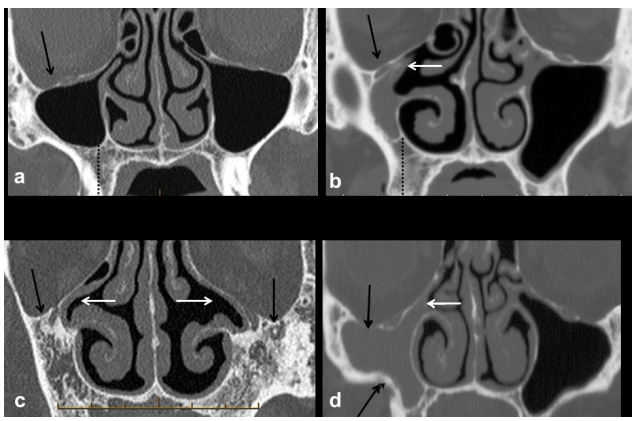

Figure 3 Hypoplasia and aplasia *versus* chronic atelectasis of the maxillary sinuses. Mild hypoplasia of the right maxillary sinus (a) is associated with a normal uncinate process and patent ostiomeatal unit; there is mild depression of the right orbital floor (black arrow). The uncinate process is hypoplastic and lateralized occluding the right infundibulum in a case of marked hypoplasia (b); the right maxillary sinus is opaque and there is asymmetric increase in height of the right alveolar process. Aplasia of the maxillary sinuses (c) associated with a lateralized and hypoplastic right uncinate process and absence of the left uncinate process (white arrows). In chronic maxillary sinus atelectasis (d), the orbital floor is inferiorly situated (black arrows) increasing orbital volume. There is contraction of the right maxillary sinus with depression of the orbital floor and retraction of the inferolateral wall (black arrows). The right infundibulum is narrow and occluded (white arrow); the absence of increase in height of the alveolar process (compare with dotted black line in a–b) confirms this as chronic maxillary sinus atelectasis (silent sinus syndrome) rather than hypoplasia.

Abnormal development

Developmental asymmetry in size and shape of the MS is common. Aplasia is extremely rare and hypoplasia is uncommon, being unilateral in 7–8% and bilateral in 2% of adults.[10,20]

The key imaging features of a hypoplastic sinus are global reduction in all dimensions and volume, **i**ncreased height of the alveolar process, a lateralized medial wall of the sinus and compensatory enlargement of the nasal cavity (Figure 3). Severe hypoplasia is associated with hypoplasia or absence of the uncinate process and a narrow infundibulum.[21] Chronic opacification of the hypoplastic sinus is therefore common secondary to occlusion of the narrow sinus ostium and infundibulum of the ostiomeatal unit.

Contraction of a normally developed sinus may occur due to chronic hypoventilation, infection, inflammation, bone dysplasia or be iatrogenic in nature, usually after surgical procedures (Figures 3 and 4). Distinction from a hypoplastic sinus is dependent on the described imaging features and especially the compensatory increase in height of the alveolar process which is seen only with a developmentally hypoplastic MS.[20–23]

Facial asymmetry is recognized in association with unilateral MS hypoplasia.[24] Posterior (enopthalmos) and inferior (hypoglobus) displacement of the globe are the most common clinical and radiological findings. The orbit (specifically the medial wall or lamina papyracea) is medialized proportional to the degree of hypoplasia. Unless recognized, this could result in inadvertent perforation of the orbit whilst performing an ethmoidectomy during endoscopic sinus surgery (ESS) for a chronically obstructed and hypoplastic MS.[25]

Craniofacial syndromes resulting in midface hypoplasia result in developmentally small maxillary sinuses. This will be bilateral in conditions such as Crouzon's and Apert's syndrome and following cleft palate repair; unilateral hypoplasia is seen in Hemifacial Microsomia (Pruzansky Grade 1) [26,27,28]

Chronic inflammation of the sinonasal mucosa during childhood can result in impaired growth of the paranasal sinuses. The volume of the maxillary sinuses decreased and the bony thickness of the sinus walls increased with longstanding paediatric chronic rhinosinusitis.[24,25]

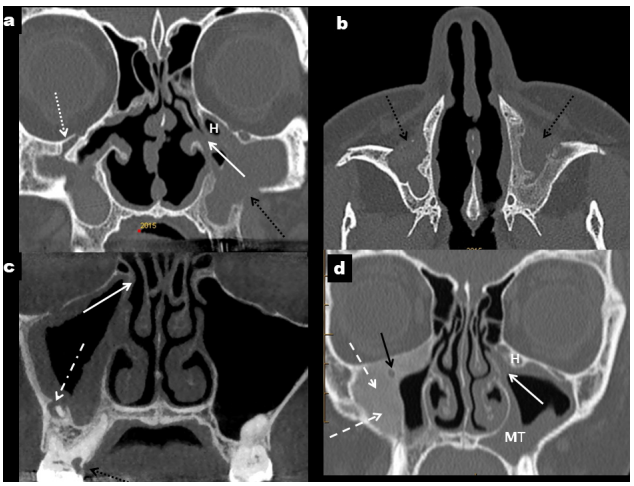

Figure 4 *Other causes of a small maxillary sinus.* Caldwell–Luc procedures (black arrows) result in thick-walled and contracted maxillary sinuses which are commonly opaque (a, b). There is depression of the orbital floor (dotted white arrow in a) and the left ostiomeatal unit is occluded (solid white arrow in a) and narrowed by an adjacent Haller cell (H). Chronic odontogenic sinusitis (c) secondary to periapical sepsis associated with 16 (dot-dash white arrow); there is peripheral mucosal thickening in a mildly contracted and thick-walled right maxillary sinus with occlusion of the ostium (white arrow). In d, peripheral bone formation with aground-glass texture typical of fibrous dysplasia (dashed white arrows) constricts the lumen of the right maxillary sinus and surrounds the infraorbital canal (black arrow). There is moderate mucosal thickening in the left maxillary sinus (MT) with occlusion of the left ostium and infundibulum (white arrow) which is narrowed by a Haller cell (H).

Genetic disorders affecting mucociliary clearance of the paranasal sinuses can lead to chronic sinusitis and, frequently, impaired sinus development. Cystic fibrosis (CF) is the most common of these conditions, it is autosomal recessive in nature and caused by one of numerous possible mutations of a gene located on chromosome 7. This results in impaired transport of chlorine out of epithelial cells, abnormally thick mucus and impaired mucociliary clearance. Secondary bacterial infection is common and the end result is chronically diseased and poorly developed paranasal sinuses.[25,29]

Imaging anatomy

Mucosa

Normal mucosa in the MS is visualized as a thin, smooth peripheral soft tissue density or signal layer on the inner surface of the sinus walls. Histologically, from outer to inner, it consists of periosteum, highly vascularized lamina propria and a thin layer of a pseudostratified columnar ciliated epithelium. Stem cells, predominantly situated in the periosteal layer, have osteogenic potential and this is thought to play a vital role in healing of bone grafts placed by sinus floor elevation procedures for augmentation of edentulous posterior maxillary segments prior to implant placement.[30]

There is extensive debate as to the thickness of the normal mucosa of the MS.[3] Most authors accept greater than 2–3 mm as pathological mucosal thickening. Mucosa in males is thicker than in females and in both sexes, mucosal thickness decreases from anterior to posterior.[31]

The cause of mucosal thickening in the inferior aspect of the maxillary sinus is commonly due to dental pathology or intervention. Periapical inflammatory lucency is the commonest overall cause in most studies, with other frequent aetiologies being advanced periodontitis, oroantral communications or fistulae and surgical procedures which result in perforation and inflammation of the MS mucosa.[3]

A clear MS with normal thickness mucosa was less common (40%) than mucosal disease within the sinus (60%) in a retrospective analysis of a large study group who underwent maxillofacial CT.[32]

Osseous

The maxillary sinus is an approximately pyramidal-shaped cavity with the base adjacent to the nasal cavity and the blunt apex pointing towards the zygoma. It has several sinus recesses: the alveolar recess pointing inferiorly, the zygomatic recess pointing laterally, a variable palatine recess (an extension of the alveolar recess) between the floor of the nasal cavity and the roof of the oral cavity and the infraorbital recess pointing superiorly bounded by the orbital surface of the maxilla.

There are six maxillary sinus walls: the superior, anterior, lateral and medial walls are broad, with narrow posterior and inferior walls.

Superior: the thin superior wall (forming most of the orbital floor), separates the contents of the orbit from the maxillary sinus. It contains the infraorbital artery and nerve (branches of the maxillary artery and maxillary division:V2, of the trigeminal nerve respectively) which enter the infraorbital groove at its posterior margin and continue anteriorly in an infra orbital canal. The anatomy of the groove and canal is variable: in a small cadaver study some orbits were found to have no groove but only a roofed canal, some to have a very thin transparent osseous roof which was termed a pseudocanal and only a minority a true groove and canal; the term infraorbital canal/groove complex (IOC/G) is therefore sometimes used.[33,34] The IOC/G courses anteriorly and slightly medially and then inferiorly towards the inferior orbital margin (Figure 5), giving origin to the anterior superior alveolar nerve and vessels,[34] 6–10 mm proximal to its exit at the infraorbital foramen (IOF).

The IOC may protrude into the anterosuperior aspect of the MS and be attached to a sinus wall by a thin septum (Figure 6). This variant is of particular importance when either open or endoscopic surgery of the MS is planned. Failure to recognize the prolapsed IOC may result in injury to the infraorbital nerve and/or artery. Prolapse of the IOC has a unilateral prevalence of 10.8% and is bilateral in 5.6%. The median distance

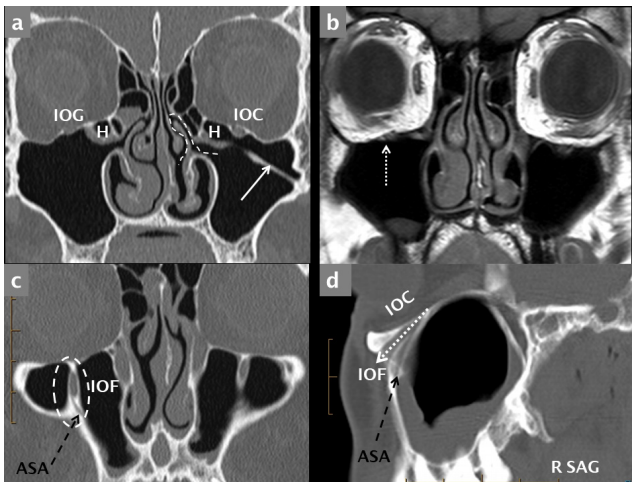

Figure 5 *Normal coronal anatomy.* Bone-window MDCT coronal reconstruction (a) and T_1 weighted coronal MRI scan (b) through the maxillary sinuses demonstrating an IOG on the right and an IOC on the left. The right infraorbital nerve and vessels are indicated (dotted white arrow) on the MRI image (b). Coronal (c) sagittal (d) reconstructions through the anterior maxilla demonstrate the IOF (dashed white oval in c) and the canaliculus sinuosus (ASA neurovascular canal, dashed black arrows). ASA: anterior superior alveolar canal; IOC: infraorbital canal; IOF: infraorbital foramen; IOG: infraorbital groove.

at which the IOC begins to protrude into the MS is 11 mm posterior to the inferior orbital rim.[35]

Blowout fractures can comminute and inferiorly displace bone fragments of the orbital floor into the maxillary sinus lumen; involvement of the thin bone medial to and involving the IOC/G complex is common. The infraorbital nerve is more susceptible to injury when not enclosed in a canal.[34,35] Other midface fractures: the Le Fort 2 and zygomatic complex fractures, also involve the orbital floor.

Anterior: the anterior wall has a mildly anteriorly concave surface and with a prominent inferolateral focal convexity, the canine eminence. The IOF is situated 5–8 mm inferior to the midpoint of the inferior orbital

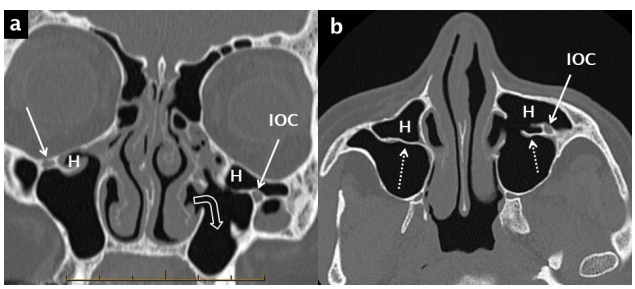

Figure 6 *Haller cells, septa and prolapse of the infraorbital canal into the maxillary sinus*. Haller cells (H) are shown on coronal (a) and axial (b) bone window reconstructions from a multidetector CT scan. These ectopic air cells narrow the diseased infundibulum bilaterally. The axial image (b) optimally demonstrates the associated septa (white dotted arrows) and the prolapse of the left infraorbital neurovascular canal (IOC) into the anterosuperior aspect of the left maxillary sinus. There has been a previous left inferior meatal antrostomy (right-angle white open arrow in a).

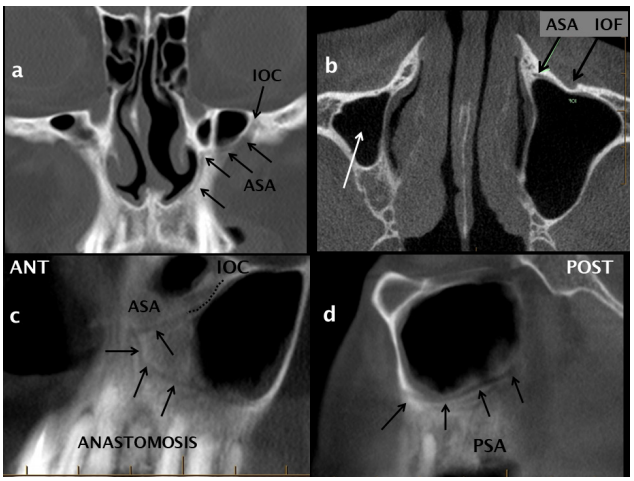

Figure 7 *The anterior superior alveolar neurovascular canal and anastomotic arcade.* The ASA neurovascular canal (canaliculus sinuosus) originates from the IOC as shown on coronal (a), axial (b) and oblique (c) reconstructions from a CBCT scan. The ASA canal courses inferiorly and medially (black arrows in *a* + c) following a sinuous course adjacent to the pyriform aperture of the nose towards the anterior maxillary teeth. The ASA and PSA neurovascular canals anastomose (c, d) to form an arcade which supplies the anterolateral sinus wall, the mucosa and the maxillary teeth. ASA:anterior superior alveolar canal; CBCT: cone beam CT; IOC: infraorbital canal; PSA: posterior superior alveolar canal

margin and is single in over 90% of subjects.[33–35] Arising from the lateral side of the IOC and then extending anteriorly, inferiorly and slightly medially, the anterior superior alveolar (ASA) canal is known as the canaliculus sinuosus and is clearly visualized by MDCT or CBCT (Figures 5 and 7).

The Caldwell–Luc procedure is the commonest external approach to the MS. It is performed by an incision in the labial sulcus of the oral vestibule superior to the canine eminence; a surgically created window in the anterior wall allows access to the MS and is commonly combined with a transnasal, inferior meatal antrostomy to encourage sinus drainage. However, mucociliary clearance always propels mucus towards the OMU and not into the surgically created fenestrations. Imaging frequently demonstrates contraction, mural thickening, opacification of the MS and occasionally mucoceles (Figure 4) as long-term complications related to mucus retention, chronic inflammation/infection and fibrous compartmentalization[20] after a Caldwell–Luc antrostomy. Surgeons still use the Caldwell–Luc procedure, or a modification utilizing an osteoplastic flap, for access to the MS to remove foreign bodies (tooth roots or implants) or mass lesions such as fungal balls (mycetoma) and odontogenic cysts or tumours.[36]

Posterior: the posterior wall is narrow and is intimately related to multiple branches of the maxillary artery and vein and several branches of the maxillary division of the trigeminal nerve (V2) within the adjacent pterygopalatine fossa (PPF). The PPF is shaped like a funnel, between the skull base superiorly and the posterior oral cavity inferiorly, with the pterygoid process (including

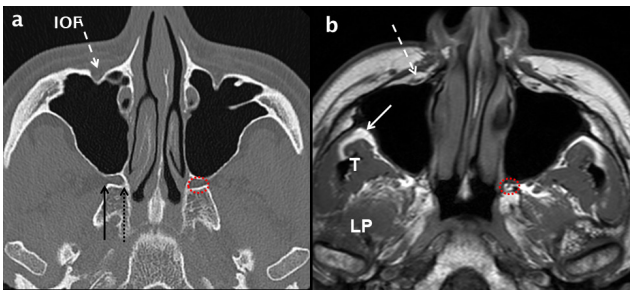

Figure 8 *Normal axial anatomy at the mid maxillary sinus level.* Comparative axial MDCT (a) and T_1 weighted MRI (b) images through the mid maxillary sinus level demonstrating bone and soft-tissue anatomy. The infra orbital neurovascular complex (white dashed arrows) is shown within the IOF. Peripheral to the lateral wall of the maxillary sinus, the infratemporal fossa (white arrow in b) is an important deep fascial space. The muscles of the medial aspect of the masticator space: temporalis (T) and LP are shown (b). The PPF (dotted red circle in a and b) contains fat, vessels and nerves. Its lateral boundary is the pterygomaxillary fissure (solid black arrow in a) which communicates with the infratemporal fossa. At the superomedial margin of the PPF is the sphenopalatine foramen (dotted black arrow in a) which is in continuity with the nasal cavity. IOF:infraorbital foramen; LP: lateral pterygoid; MDCT: multidetector CT; PPF: pterygopalatine fossa.

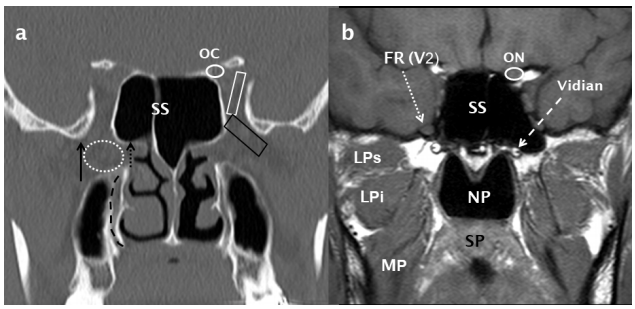

Figure 10 *Normal coronal anatomy through the pterygopalatine fossa.* A coronal bone-window MDCT image (a) shows the PPF (dotted white oval) and its lateral (pterygomaxillary fissure: black arrow) and medial (sphenopalatine foramen: short dotted black arrow) boundaries. The inferior orbital fissure (black trapezoid) and superior orbital fissure (white trapezoid) are also indicated. The descending palatine canal is indicated by a curved, dashed black line. Directly posterior to the PPF, a T_1 weighted MRI image (b) demonstrates the FR (dotted white arrow) containing the V2 nerve and also the Vidian canal (dashed white arrow). The ON (b) is shown in the OC (a) and the NP, SP, MP and the superior and inferior heads of LP (LPs and LPi respectively) are indicated (b). LP: lateral pterygoid; MP: medialpterygoid; NP: nasopharynx; OC: optic canal; ON: optic nerve; SP:soft palate.

the pterygoid plates) and the anterior portion of the greater wing of the sphenoid bone forming the posterior margin (Figures 8 and 9). Other important contents of the PPF include the pterygopalatine ganglion which receives pre-ganglionic parasympathetic fibres from the facial nerve via the nerve of the Vidian (pterygoid) canal and post-ganglionic sympathetic fibres from the internal carotid artery plexus.

The PPF communicates with the infratemporal fossa laterally via the pterygomaxillary fissure, the nasal cavity medially via the sphenopalatine foramen, the palate and oral cavity inferiorly via the greater and lesser palatine canals and foramina, the orbit superiorly via the posterior half of the inferior orbital fissure and the middle cranial fossa via the foramen rotundum (containing V2) (Figures 8–10).

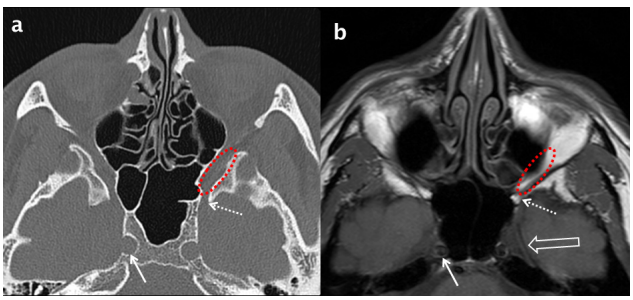

Figure 9 *Normal axial anatomy at the superior margin of the maxillary sinus*. Comparative bone window MDCT (a) and T_1 weighted MRI (b) axial images through the superior aspect of the maxillary sinuses. Inferiorly, the inferior orbital fissure (dotted red oval) is contiguous with the PPF and posteriorly with the foramen rotundum (dotted white arrows). Meckel's cave (open white arrow in b) and the internal carotid artery (white arrows) are also demonstrated. PPF: pterygopalatine fossa; MDCT: multidetector CT.

The clinical importance of the PPF is that it acts as a conduit for tumour and sepsis to spread from the maxillary sinus and oral cavity into adjacent, critical anatomical structures. Fat within the fossa, which is clearly visible on CT and MRI (but not CBCT), allows detection of subtle neoplastic infiltration.

Lateral: the lateral wall, facing posterolaterally towards the infratemporal fossa, is thin and is contiguous inferiorly with the buccal aspect of the alveolar ridge. The lateral wall contains the PSA canal, an important structure when considering the site and design of a flap for sinus augmentation (Figure 11).

Mucosal thickening within the sinus commonly leads to thickening and sclerosis of this sinus wall, which may be of significance when performing sinus augmentation (Figures 4c, 8c and d). In addition, perforation of the Schneiderian membrane during elevation is more likely to occur with thin mucosa (<3 mm). Thicker mucosa is more resilient to instrumentation.[37,38]

The infratemporal fossa lies peripheral to the lateral antral wall and is an important deep fascial space which can be involved by spread of infection or tumour and this also requires CT or MRI for assessment rather than the extremely limited soft tissue contrast of CBCT. Expansile odontogenic cysts and tumours can also extend into the adjacent fat of the infratemporal fossa (Figure 12).

Medial: the medial wall of the MS also forms the lateral wall of the nasal cavity. The main MS ostium is situated superiorly in the medial wall at or just inferior to the level of the orbital floor. MS ostia are discussed further in the section on the ostiomeatal unit. It is useful to divide the medial wall into unequal thirds: the upper third extends from the ostium above to the level of attachment of the inferior turbinate to the lateral nasal

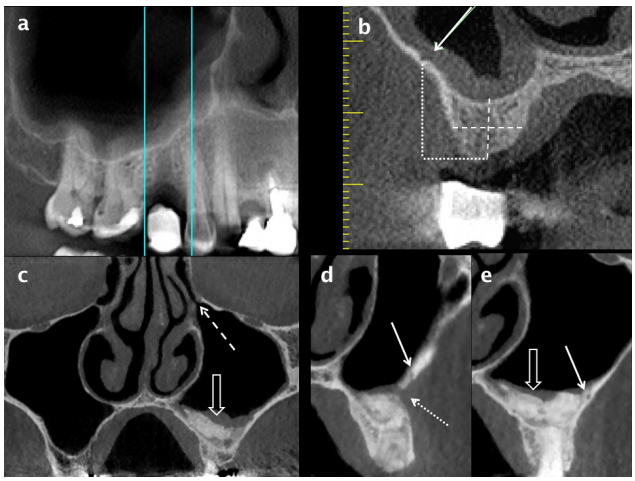

Figure 11 *Assessment for implant placement in the posterior maxilla using CBCT.* A panoramic reconstruction of the right posterior maxillary quadrant (a) shows a stent marker indicating the proposed site for implant placement in the 15 region and the location of radial reconstructions. The height and width (dashed white lines) of alveolar bone can be measured on a radial reconstruction through the mid-point of the edentulous segment (b). The position of the PSA canal is indicated by a white arrow; it is in a submucosal position and just less than 1 mm in diameter. The height of the PSA from the alveolar crest can be measured (dotted white lines). A sinus lift procedure and guided bone regeneration in the left posterior maxilla are shown on coronal (c) and radial (d, e) reconstructions from a CBCT scan. Mild mucosal thickening overlies the consolidated bone graft (open white arrow in a) and the left OMU (dashed white arrow) is patent. The surgical cut for the bone window (dotted white arrow in d) and a tiny intraosseous PSA (solid white arrow in d and e) are shown. CBCT: cone beam CT; OMU: ostiomeatal unit; PSA: posterior superior alveolar.

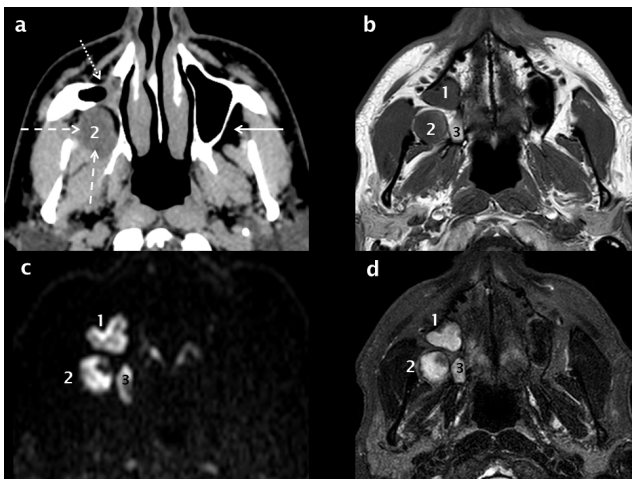

Figure 12 *MRI and the detection of recurrent OKC.* The right maxillary sinus is contracted (white dotted arrow) secondary to a previous Caldwell–Luc procedure for excision of a right posterior maxillary OKC as seen on an axial soft-tissue window MDCT reconstruction (a). There is recurrent OKC in the right infratemporal fossa (white dashed arrows, 2); this would be difficult if not impossible to visualize on CBCT. T1 (b) and fat-saturation T2 (d) axial MRI scans demonstrate two additional recurrent lesions (1 + 3). All three lesions (1, 2 + 3) demonstrate restricted diffusion (high signal foci in c) which is virtually pathognomonic of an OKC. CBCT: cone beam CT; OKC: odontogenickeratocysts.

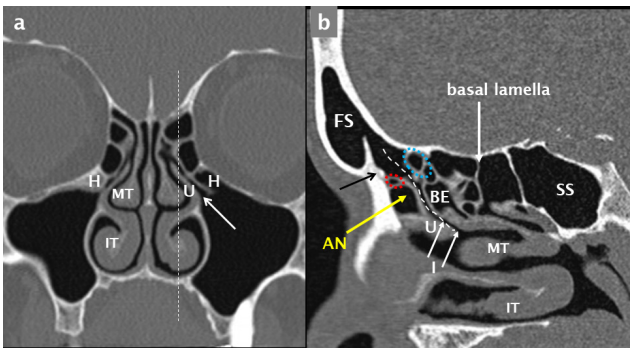

Figure 13 Anatomy of the FR and OMU. A coronal MDCT reconstruction (a) at the level of the mid-OMU; the ostium and infundibulum (white arrows) and bilateral Haller cells (H) are indicated. The plane of the sagittal reconstruction is shown by the white dashed line in a. The FR drains into the infundibulum (dashed white curvilinear line) as seen on this para-sagittal reconstruction through the left FR and mid-OMU (b). Key anatomical landmarks include the IT, MT, ,U, AN cell situated anterior to the FR and the BE situated posterior to this drainage channel. The frontal beak (black arrow in b) is a prominent ridge of bone that separates the FS from the FR and corresponds to the frontonasal junction. Ectopic anterior ethmoid air cells may be situated superior to the AN and anterior to the FR (small dotted red oval) or superior to the BE and posterior to the FR (small dotted blue oval). When large, they narrow the FR and predispose to frontal sinusitis. The basal lamella is the coronal attachment of the MT and divides the ethmoid sinus into anterior and posterior air cells. The sphenoid sinus (SS) is also indicated. AN: agger nasi; BE: bulla ethmoidalis; FR: frontal recess; FS: frontal sinus; IT: inferiorturbinate; MT: middle turbinate; OMU: ostiomeatal unit.

wall below, the larger middle third extends between this attachment and the floor of the nasal cavity, and a variable-sized lower third forms the medial wall of the alveolar recess below the level of the nasal floor (Figure 13a).

Inferior: the inferior wall, or sinus floor, is contiguous with the alveolar process and contained roots of the maxillary dentition. The anteroposterior extent of the sinus, location and morphology of septa, width and shape of the alveolar recess and the relationship of the maxillary tooth root apices to the sinus floor are all relevant features when assessing patients for extraction of posterior teeth, sinus augmentation and potential implant placement.

Extent—the anterior and posterior margins of the MS are most commonly located in the first premolar (49%) and second molar (84%) regions respectively.[12,39,40] When extensively pneumatized, the anterior recess of the sinus may extend to the canine apex and this is associated with medial extension of a palatine recess between the palate and the floor of the nasal cavity (Figure 2d). Significant asymmetry of the extent of pneumatisation of the MS is seen in 17% of patients.[10,18,41]

Septa—maxillary sinus septa are thin, linear or curvilinear plates of cortical bone which usually arise from the sinus floor. Septa are common and their frequency is underestimated on dental panoramic tomography (DPT). Multiplanar analysis of a volumetric data set derived from MDCT or CBCT is the only accurate way to evaluate septa as well as the sinus floor in general. The

Figure 14 *Maxillary sinus septa and ridges*. Septa arising from the inferior wall of the maxillary sinuses are shown on a cropped dental panoramic tomograms (white arrows in a), oblique sagittal (white arrow in b) and cropped panoramic reconstructions from CBCT (white arrow in c). A thicker and shorter inferior sinus ridge overlies the 17 region in b (dashed white arrow) and the alveolar recess of the right maxillary sinus extends towards the ridge crest in the edentulous 16 region (dotted white arrow). CBCT: cone beam CT.

septal shape has been described as an inverted gothic arch arising from the inferior or inferolateral walls of the sinus; they are coronal or oblique in orientation and project superiorly [12,41,42] (12, 20 and 42).

Septa may be primary (developmental) or secondary (acquired). Primary septa are seen in dentate patients and most commonly occur as a large septum overlying the apices of the first and second molars and smaller septa in the premolar and third molar regions (Figure 14). Secondary septa are related to tooth loss and therefore seen in partially dentate patients. Tooth loss leads to resorption of the alveolar bone height from the oral side and focal descent of the sinus floor secondary to activity of osteoclasts in the Schneiderian membrane causing focal excavation of the alveolar process.[43] Secondary septa usually represent residual bone or a pre-existing ridge in the sinus floor on either side of focal alveolar bone loss; this is most common in the first molar region (Figure 14b).

The main conclusions of multiple studies[41,42,44] evaluating sinus septa are:

a. Primary and secondary septa are common, being seen in 50% of dentate and edentulous posterior maxillary segments.
b. Septa found in the edentulous maxilla are shorter than those found in dentate patients.
c. Some authors consider a septum to be greater than 2.5 mm in height; shorter septa are better described as ridges.
d. The presence of septa increases the risk of mucosal perforation during a sinus lift procedure.
e. The presence of septa is associated with thinner sinus mucosa.

Maxillary sinus septa are also seen in the anterosuperior aspect of the sinus in association with laterally situated ectopic anterior ethmoid air cells (Haller cells) as well as occasional prolapse of the IOC into the sinus (Figure 6). They constitute 23% of all MS septa.[35,42]

Alveolar Recess—The alveolar recess varies in shape, depth and width. This is of practical importance as these factors determine the ease of performing a sinus lift procedure and the risk of complications.

Small maxillary sinuses tend to be round in shape with a smooth, round or flat floor and shallow alveolar recess. In less than 40% of the population, the MS has a larger alveolar recess with an irregular inferior contour as the sinus extends between the molar and premolar tooth roots and apices.[12] This creates elevations in the floor of the maxillary sinus as seen on DPT, so called "hillocks".[45]

In comparative studies, the depth of the alveolar recess is measured with reference to the floor of the nasal cavity using coronal reconstructions from CT or CBCT. The larger the MS (increased volume and height) the greater the depth of the recess. In most adults, the floor of the alveolar recess is situated about 3–5 mm inferior to the nasal floor.[12] In 20% of adults the most inferior part of the MS is above the nasal floor, in 15% it is situated at the same level as the nasal floor.

The width of the alveolar recess has been assessed using coronal reconstructions from CBCT. One study measured the transverse dimension (width) at specific heights corresponding to the inferior (2.3 mm superior to the MS floor) and superior (15 mm superior to the crest) boundaries of the bone window used for a sinus lift procedure. Narrow, average, or wide sinuses were classified when the alveolar recess width was <8, 8–10 and >10 mm at the inferior boundary or <14, 14–17 and >17 mm at the superior boundary, respectively.[46]

The alternative technique is to measure the angle of the alveolar recess.[31] This is the angle at the apex of an inverted triangle formed by the most inferior point of the alveolar recess and points on the mucosal surface of the buccal and palatal walls, 10 mm superior to the sinus floor. The average angle is 73°; a low angle is designated as ≤ 65°, intermediate at 65 to 80° and a high angle as greater than 80°.

The angle and width of the recess increase from mesial to distal and tend to be higher in males reflecting the gender difference in sinus size. There is an increased risk of mucosal perforation of the mucosa during a sinus lift when the alveolar recess is narrow, as measured by the width or angle.

Alveolar Process—CBCT and (less often) MDCT are frequently used to evaluate the height, width and quality of alveolar bone within a proposed site for implant placement.[46] Cortical integrity and the shape of the superior margin of the alveolar process, which forms the inferior wall of the maxillary sinus, are also assessed.

Height: defined as the distance from the alveolar crest to the cortical margin of the floor of the maxillary sinus

(Figure 11a,b). Overall, alveolar bone height decreases distally from the premolar to the molar region in both dentate and edentulous segments (Figures 13 and 14) with the reduction in height being more marked in edentulous segments.[12,47]

Width: the buccopalatal width (including the cortices) may be uniform throughout an edentulous segment but as resorption of unloaded bone is most marked at the alveolar crest, this can result in a relatively narrow orpointed ridge. This is more common in the anterior maxilla but can involve the premolar region. In these cases, the minimum buccopalatal width is the crucial factor in deciding the proposed implant width and whether buccal augmentation needs to be performed, with or without a sinus lift procedure (Figure 11).

Quality: assessment of bone quality prior to implant placement is by a combination of visual assessment and quantitatively by measurement of bone density based on the degree of attenuation of the X-ray beam.[47]The unit of measurement is the Hounsfield unit (HU) which is standard on all CT (MDCT) systems. In contrast, the displayed grey scale levels in CBCT systems are arbitrary and non-uniform between different vendors such that the ability to assess the quality and density of bone is limited.[39] Recent *in vitro* research using a phantom containing eight materials of known density as the reference, demonstrated that conversion factors can be derived for any CBCT scanner to convert the grey scale into accurate HU values.[48]

Maxillary dentition: the apices of the posterior maxillary teeth have a variable relationship to the floor of the MS (Figure 15). Due to the superimposition evident in DPT, apical penetration of the sinus lumen is commonly overdiagnosed.[45,49,50] In one comparative study, apical penetration of the sinus was suspected in 50% of cases when evaluated by DPT as compared to 27% when the same study group was evaluated by cross-sectional imaging.[48] In contrast, when the MS is small and the alveolar recess does not descend below the nasal floor, DPT correlates closely with cross-sectional imaging.[40,50]The exact relationship of the apices to the alveolar recess and sinus floor is important when procedures or endodontic treatment of posterior maxillary teeth are considered.

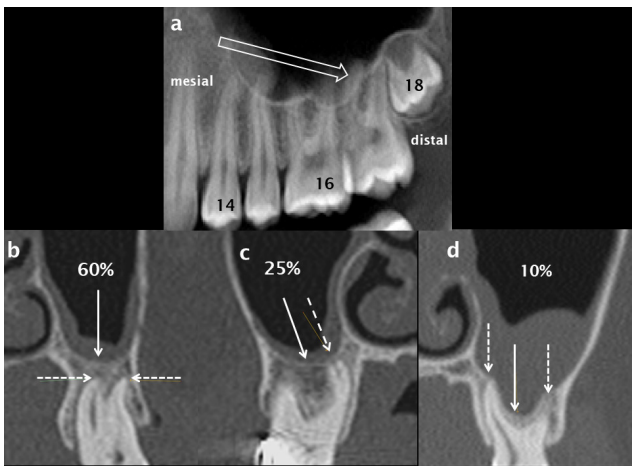

Figure 15 *The relationship of the apices of the posterior maxillary teeth to the maxillary sinus.* Alveolar height decreases from mesial to distal (open white arrow) in the left posterior maxillary quadrant as shown on a panoramic CBCT reconstruction (a). In 35% of cases the apices of the maxillary molars (dashed white arrows) are intimately related to the floor of the maxillary sinus (solid white arrows); they either abut the sinus floor (c) or the sinus floor extends inferiorly between the apices/roots (d). In 60% of cases, the apices are inferior to and separate from the floor of the sinus (b). CBCT: cone beam CT.

Multiple studies using CBCT have evaluated of the relationship of the maxillary posterior tooth root apices to the floor of the MS.[12,40,41,45,50–52] A representative study demonstrated an intimate relationship in 35% of the study group.[51] In 25%, the sinus floor was at the level of the apices as seen on coronal reconstructions and in 10% of patients the floor extended inferior to the level of the apices, usually between rather than surrounding the roots. In the remaining 65% of cases, the sinus floor was superior to the apices (Figure 15). The average distance between the sinus floor and apices was 7 mm in the first premolar region and 2 mm in the second molar region, with the shortest distance overlying the distobuccal apex of the second molar. At least two studies have shown that the mean distance from the apices to the floor of the MS decreased with increasing age.[50]

In contrast, studies using CBCT and CT have shown the buccal apices of the first premolars are closest to the buccal alveolar wall, when compared to the largest mean distance of 4.5 mm in the second molar region.[52] This is relevant if an apicectomy is planned.

There is a positive correlation between the length of root projection into the maxillary sinus as observed on a DPT and the degree of focal descent of the sinus floor towards the alveolar crest that occurs following extraction within the edentulous space. Recent CBCT studies demonstrate that at posterior maxillary extraction sites, focal pneumatization corresponds to about 30% of loss of height and socket remodelling to 70% of the loss of alveolar height. Loss of ridge height is most marked in the first molar region and can be largely prevented by socket preservation techniques.[43]

The ostiomeatal unit/ ostiomeatal complex

The terms ostiomeatal unit (OMU) and ostiomeatal complex are used interchangeably to describe the common drainage of the anterior sinuses. This is a functional unit, rather than a precisely defined anatomical term. The OMU comprises the MS ostium, ethmoidal infundibulum, uncinate process, hiatus semilunaris, middle meatus, anterior ethmoid air cells and the frontal recess, the latter being the drainage channel of the frontal sinus (Figures 1 and 3). Diseased mucosa in the ethmoidal infundibulum impairs ventilation and mucociliary clearance of all three anterior sinuses.

Functional endoscopic surgery, or more simply endoscopic sinus surgery (ESS), is the principal technique

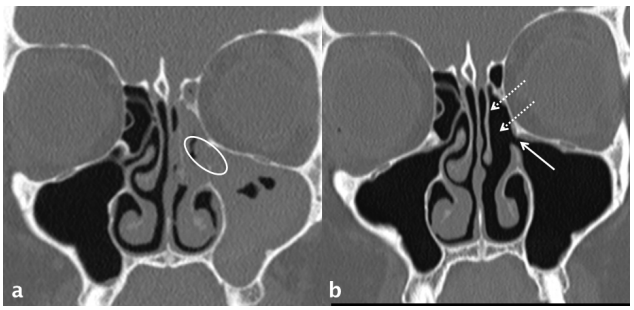

Figure 16 Left OMU pattern of sinusitis and successful ESS. The left OMU is occluded (white oval in a) and there is subtotal opacification of the maxillary and ethmoid sinuses on this side. Following ESS which includes a left anterior ethmoidectomy (dotted white arrows in b) and uncinectomy, there has been marked improvement: the antrostomy is patent (white arrow in b) and the ethmoid and maxillary sinuses are now clear. ESS, endoscopic sinus surgery; OMU, ostiomeatal unit.

used to treat chronic rhinosinusitis which is refractory to medical treatment. The aims of ESS are to re-establish normal ventilation, mucociliary clearance and sinus drainage.[2,53]

To improve drainage of the anterior sinus group, an endoscopic anterior ethmoidectomy and resection of the uncinate process are performed (Figure 16).

An intimate knowledge of the anatomy of the ethmoid bone and the multitude of normal variants that occur in this region are essential both for the surgeon and radiologist reporting the pre-operative CT scans which act as aroadmap for surgical planning.[54–56]

Understanding the basic anatomy and function of the OMU is therefore of therefore important to the dental and maxillofacial radiologist reporting CBCT or CT where the primary focus is the maxilla or MS. It is not as simple as commenting that the MS ostium is patent or occluded.

Although multiplanar analysis from the volumetric data set is always undertaken, the anatomy and patency of the OMU is best assessed on coronal reconstructions. Mucus swept by ciliary action from the MS passes through the following passages (Figure 1).

Ostium: the ostium of the MS is situated on the superior aspect of the medial wall of the sinus just below the level of the orbital floor; the mean distance from the sinus floor to the ostium being 29 mm.[57] It is oval or slit-shaped and orientated horizontally or obliquely with a diameter of 3–10 mm.[54] In the coronal plane, 70 to 80% of ostia are situated at or posterior to a reconstruction midway between the anterior and posterior walls of the MS at the approximate coronal level of the first maxillary molar.[54,57]

Accessory ostia arise in the thin, membranous portion of the medial wall of the maxillary sinus, usually postero inferior to the main ostium. They are seen in 20–40% of the population. They may be acquired rather than developmental, the thin membranous portion rupturing as a result of maxillary sinusitis and obstruction of the main ostium.[54,57]

Infundibulum: mucus then passes into the second passage, the narrow slit-like ethmoidal infundibulum. In the coronal plane, the infundibulum is angulated superomedially with the uncinate process of the ethmoid bone as its medial boundary and the anterior ethmoid air cells and medial orbital wall (lamina papyracea) situated superolaterally (Figure 1).

Three-dimensional (3-D) anatomy is more complex: the uncinate process is a crescent-shaped extension of the ethmoid bone which arises anterosuperiorly and extends posteroinferiorly to attach to the medial maxillary wall, inferior to the sinus ostium. The infundibulum is best described as being shaped like a curvilinear funnel with the opening of the funnel being situated anterosuperiorly. It requires an uncinectomy to be visualized by the endoscopic sinus surgeon (Figures 13 and 16).

Hiatus semilunaris: the hiatus semilunaris is situated at the superomedial margin of the infundibulum and therefore has the same curvilinear shape and oblique orientation in the sagittal plane. It is situated anteroinferior to the most prominent and largest anterior ethmoid air cell, the bulla ethmoidalis (Figure 1).

Middle meatus: this passage receives mucus from the MS as well as from the multiple small ostia of anterior ethmoid air cells which are uncommonly visualized on imaging. Mucus from the frontal sinus has a variable drainage into either the infundibulum or directly into the middle meatus. The lateral and medial boundaries of the middle meatus are the uncinate process and the middle turbinate respectively (Figure 1).

Anterior ethmoid air cells: the multiple air cells making up the ethmoid labyrinth or sinus are divided anatomically into anterior and posterior groups by the basal lamella, which is the coronal attachment of the middle turbinate (Figure 13b), which is best seen on sagittal reconstructions.

There are normal and variant anterior ethmoid air cells which are frequently discussed in the rhinology and radiology literature[54–56] :

Ethmoidal bulla—the largest and most prominent anterior ethmoid air cell is an important anatomical landmark. It forms the posterior and superior boundary of the ethmoidal infundibulum (Figures 1 and 3).

Agger nasi cell—the most anterior ethmoid air cell lies anterior and inferior to the frontal recess. It is not confined to the ethmoid bone and extends anteriorly into the lacrimal bone. It is almost always present (95%)[55] and varies in size (Figure 13b).

Haller (infraorbital) air cells—these are present in up to 45% of the population[54] and are situated inferolateral to the ethmoidal bulla, extending along the medial aspect of the orbital floor, superior to the ethmoidal infundibulum. Haller cells frequently lead to narrowing of the infundibulum, which may become occluded, especially if the Haller cell is infected (Figures 13 and 17). Of the anterior ethmoid variant air cells, Haller cells are the most commonly visualized utilizing the field of view used for CBCT performed for implant planning.

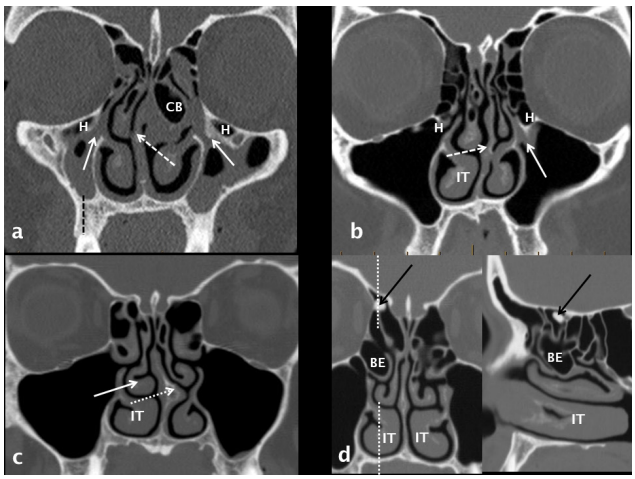

Figure 17 *Anatomical variants which narrow the OMU and may predispose to sinusitis.* The right maxillary sinus is hypoplastic with increase in height of the alveolar process (dashed black line). Both OMU's are diseased and occluded (white arrows) with bilateral ethmoid and maxillary disease. Significant anatomical variants include bilateral H cells, septal deviation to the right (dashed white arrow) and a left CB. The infundibulum of the left OMU is occluded (white arrow) and narrowed by a H cell and septal deviation to the left (white dashed arrow). The right IT is enlarged. There is septal deviation to the left, a left-sided septal spur (dotted white arrow), paradoxical curvature of the right middle turbinate (solid white arrow) and hypertrophy of the right IT. Coronal and right para-sagittal reconstructions demonstrate a large right BE and hypertrophy of the IT. An incidental osteoma (black arrow) is noted in the right anterior ethmoid region. H: Haller cell; BE, bulla ethmoidalis; CB: concha bullosa; IT: inferior turbinate; OMU: ostiomeatal unit.

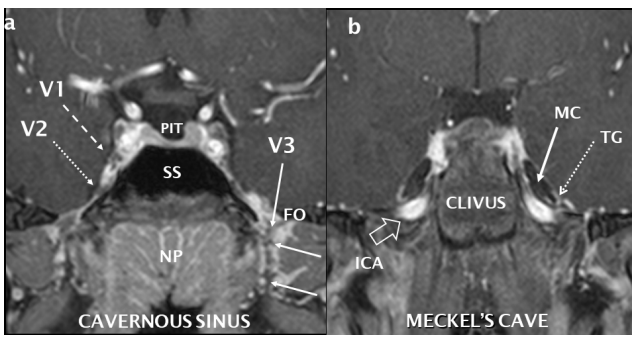

Figure 18 *Normal coronal anatomy of the central skull base and trigeminal nerve.* Post-gadolinium T1 coronal fat saturation, high resolution sequence performed at 3 Tesla with reconstructions through the cavernous sinus (a) and further posteriorly through Meckel's cave (b). The normal right V1 (dashed white arrow) and V2 (dotted white arrow) nerves are seen as low signal structures surrounded by the vividly enhancing cavernous sinus. Other cranial nerves are visible. The left V3 is seen (white arrow) as it exits through the FO surrounded by an enhancing perineural vascular plexus. Where PIT = pituitary, SS = sphenoid sinus and NP = nasopharynx. The cerebrospinal fluid-filled Meckel's cave (MC: solid white arrow) contain the U-shaped and enhancing trigeminal ganglion (TG: dotted white arrow). High signal flowing blood is seen in the ICA as it extends superiorly into the foramen lacerum (open white arrow). FO: foramen ovale; ICA: internal carotid artery.

Uncinate process variations—a lateralized uncinate process narrows the infundibulum, which is then more prone to become occluded when an inhaled infective agent or irritant leads to mucosal thickening. Lateralization occurs on the same side as a hypoplastic sinus and is also associated with pneumatization and expansion of the middle turbinate (concha bullosa) as well as deviation of the nasal septum to the ipsilateral side. Commonly, a bony septal spur can occur on the same side to which the septum deviates (Figure 17).

Frontal recess: this represents the drainage channel of the frontal sinus and has previously been called the frontonasal or nasofrontal duct (these terms have been abandoned, since this is not a true duct).[54,56] The frontal recess opens into either the ethmoidal infundibulum or the middle meatus depending on the antero superior attachment of the uncinate process. Most commonly this attachment is lateral, to the medial orbital wall (lamina papyracea) or the adjacent agger nasi air cell, and mucus then drains directly into the middle meatus. Less commonly, mucus from the frontal recess drains inferolaterally into the infundibulum when the uncinate process attaches either superiorly, to the anterior skull base, or superomedially to the lamella of the middle turbinate. Frequently, a combination of superior uncinate process attachments is present.

There are several ectopic anterior ethmoid air cells which extend anterosuperiorly from the anterior ethmoid labyrinth and may lead to narrowing of the frontal recess and recurrent frontal sinusitis. They are classified according to their position, anterior or posterior to the frontal recess, and are optimally assessed on sagittal reconstructions (Figure 13b). Because of their position, they are difficult to treat using the small, fixed endoscopes employed in ESS.

Innervation and vascular supply

The MS, alveolar process and dentition share common, innervation, arterial supply, and venous and lymphatic drainage. The nerves and arteries occupy the same osseous channels and foramina, sharing the same anatomical name.

Sensation: general sensation is supplied by the maxillary division of the trigeminal nerve (V2). After leaving the trigeminal ganglion in Meckel's cave, V2 passes anteriorly along the inferolateral wall of the cavernous sinus, exits the cranial cavity via the foramen rotundum and enters the superior part of the PPF (Figure 17). The main trunk of the nerve continues anteriorly as the infraorbital nerve within the IOC/G of the superior wall of the maxillary sinus before exiting at the infra orbital foramen to supply the nose, cheek, upper lip and lower eyelid (Figures 5, 8 and 10). V2 and its major branches are clearly seen on high resolution MRI performed at a high field strength (optimally 3 T). Asymmetric loss of perineural fat, enlargement and enhancement of the involved nerve are all signs of large nerve perineural involvement by tumour, a highly important prognostic

factor. MDCT is less sensitive in this regard and CBCT will only demonstrate enlargement or demineralisation of the neural canal which is only seen in advanced or longstanding perineural malignancy.

The PSA nerve originates from the maxillary division (V2) within the inferior orbital fissure just before it enters the IOC/G. Passing inferiorly along the infratemporal surface of the maxilla, the PSA nerve gives off several small branches to the gingiva and buccal mucosa before entering the PSA canal to supply the molars. The middle superior alveolar nerve is present in 30–72% of the population[58] and like the anterior superior alveolar nerve; it arises from the IOC/G in the orbital floor. The superior dental plexus has input from all the superior alveolar nerves and supplies the incisor, canine, premolar and first molar teeth, gingivae, maxillary sinus mucosa and the antero inferior nasal cavity. The plexus is not visible on imaging.

Arterial supply: the principal arterial supply of the maxillary sinus is provided by the posterior superior alveolar and infraorbital arteries supplemented by the greater palatine and sphenopalatine arteries. All vessels are branches of the maxillary artery, the larger terminal branch of the external carotid artery.[59]

The design of the lateral approach for augmentation of the atrophic alveolar ridge by a sinus floor elevation (lift) procedure, should take into account the important arterial anastomosis of the PSA and infraorbital arteries.[59–61] This anastomosis forms a vascular arcade supplying the Schneiderian membrane and the anterolateral wall of the MS; it can be demonstrated on oblique reconstructions from CT or CBCT (Figure 7). Haemorrhage from inadvertent arterial transection leads to operative and post-operative complications including tearing of the sinus mucosa due to impaired visualization, submucosal or intrasinus bleeding and oedema, graft failure, occlusion of the sinus ostium and secondary acute sinusitis.[44]

In a cadaveric study, the PSA-anastomosis measured 2 mm or less in 97% of cases and was larger in males and with increasing age.[59,60] A recent meta-analysis demonstrated a significantly higher detection rate of the anastomosis for CBCT of 78% as compared with 51% for MDCT.[59,60] Smaller vessels were detected by CBCT reflecting the higher spatial resolution of this technique.

The arterial anastomosis, which predominantly represents the PSA in the premolar and molar region, may be intraosseous, submucosal (deep to the Schneiderian membrane) or occasionally subperiosteal in location. In the second molar to second premolar region, the anastomosis is most commonly partially intraosseous and submucosal[59] which results in a shallow medial osseous groove of the infero-lateral osseous wall of the maxillary sinus (Figure 11). The distance of the PSA-anastomosis superior to the crest reduces from the premolar to the molar region and this is most marked in edentulous and atrophic segments. The mean vertical distance between the PSA canal and alveolar crest in the first molar region is widely accepted as 15 mm.[59,60]

For optimal surgical assessment, the arterial anastomosis should be identified and its position documented with the highest possible resolution using CBCT. Vessels not detected by CBCT are likely to be extremely small and less clinically relevant.[61]

Discussion

Widespread use of high resolution, multiplanar CBCT by the dental profession has revolutionized the study of the maxillofacial region. This is especially true in the maxilla where there is an intimate relationship of the posterior teeth within the alveolar process to the MS. It is analogous to the introduction and continued development of CT and subsequently MRI that changed the practice of otolaryngology and head & neck radiology.

With regard to the MS, the focus of dental and maxillofacial imaging has been on the relationship of dental pathology and surgical procedures to mucosal disease in the alveolar recess of the sinus; the importance of more extensive opacification and of a patent sinus ostium is now well recognized. In contrast, the primary focus for the general radiologist or rhinologist assessing a patient with disease of the MS, is to confirm the patency of the OMU, whether the anterior ethmoid and frontal sinuses are also diseased and the presence of significant anatomical variants that may narrow the anterior drainage channels or influence endoscopic surgery.

It is vital that radiologists who report imaging that includes the MS have an understanding of basic sinonasal physiology, bone and soft-tissue anatomy, rhinosinusitis, dental disease and common surgical procedures. There is overwhelming evidence that dental disease, surgical intervention and complications are the usual cause of mucosal thickening in the inferior aspect of the maxillary sinus, often asymptomatic and frequently diagnosed on CBCT or CT.

In contrast, sinusitis is a clinical diagnosis that may be supported by imaging findings. According to recent data, 25–40% of sinusitis that involves the anterior paranasal sinuses, including the maxillary sinus, has an odontogenic cause. The importance of assessment of the maxillary dentition whilst interpreting sinonasal CT and MRI has received scant attention in the head and neck radiological literature. A recent review article has addressed this topic and proposes a checklist for interpreting sinonasal CT which includes routine review of the maxillary dentition.[3]

Acknowledgment

We would like to thank the radiographers at Perth Radiological Clinic and their ongoing commitment to excellence in the fields of sinonasal and maxillofacial imaging.

References

1. Krouse JH. The unified airway. *Facial Plast Surg Clin North Am* 2012; **20**: 55–60. doi: https://doi.org/10.1016/j.fsc.2011.10.006
2. Weber RK, Hosemann W. Comprehensive review on endonasal endoscopic sinus surgery. *GMS Current Topics in Otorhinolaryngology - Head and Neck Surgery* 2015; **14**.
3. Whyte A, Boeddinghaus R. Imaging of odontogenic sinusitis. *Clin Radiol* 2019; **74**: 503–16. doi: https://doi.org/10.1016/j.crad.2019.02.012
4. Cohen NA. Sinonasal mucociliary clearance in health and disease. *Ann Otol Rhinol Laryngol* 2006; **115**(9_suppl): 20–6. doi: https://doi.org/10.1177/00034894061150S904
5. Bustamante-Marin XM, Cilia OLE, Clearance M. *Cold Spring Harb Perspect Biol* 2018; **9**.
6. Beule AG. Physiology and pathophysiology of respiratory mucosa of the nose and the paranasal sinuses. *GMS Curr Top Otorhinolaryngol Head Neck Surg* 2011; **2010**.
7. Gudis D, Zhao K-Q, Cohen NA. Acquired cilia dysfunction in chronic rhinosinusitis. *Am J Rhinol Allergy* 2012; **26**: 1–6. doi: https://doi.org/10.2500/ajra.2012.26.3716
8. Dykewicz MS, Hamilos DL. Rhinitis and sinusitis. *Journal of Allergy and Clinical Immunology* 2010; **125**: S103–S115. doi: https://doi.org/10.1016/j.jaci.2009.12.989
9. Lorkiewicz-Muszynska D, Kociemba W, Rewekant A, Sroka A, Jonczyk-Potoczna K, Patelska-Banaszewska M, et al. Development of the maxillary sinus from birth to age 18. *Postnatal growth patterns. International Journal of Paediatric Otorhinolaryngology* 2015; **79**: 1393–400.
10. Scuderi AJ, Harnsberger HR, Boyer RS. Pneumatization of the paranasal sinuses: normal features of importance to the accurate interpretation of CT scans and MR images. *American Journal of Roentgenology* 1993; **160**: 1101–4. doi: https://doi.org/10.2214/ajr.160.5.8470585
11. Przystańska A, Kulczyk T, Rewekant A, Sroka A, Jończyk-Potoczna K, Gawriołek K, et al. The association between maxillary sinus dimensions and midface parameters during human postnatal growth. *Biomed Res Int* 2018; **2018**: 1: 10: doi: https://doi.org/10.1155/2018/6391465
12. Lovasova K, Kachlik D, Rozpravkova M, Matusevska M, Ferkova J, Kluchova D. Three-Dimensional CAD/CAM imaging of the maxillary sinus in ageing process. *Ann Anat* 2018; **218**: 69–82. doi: https://doi.org/10.1016/j.aanat.2018.01.008
13. Bhushan B, Rychlik K, Schroeder JW. Development of the maxillary sinus in infants and children. *Int J Pediatr Otorhinolaryngol* 2016; **91**: 146–51. doi: https://doi.org/10.1016/j.ijporl.2016.10.022
14. Ariji Y, Kuroki T, Moriguchi S, Ariji E, Kanda S. Age changes in the volume of the human maxillary sinus: a study using computed tomography. *Dentomaxillofac Radiol* 1994; **23**: 163–8. doi: https://doi.org/10.1259/dmfr.23.3.7835518
15. Przystańska A, Kulczyk T, Rewekant A, Sroka A, Jończyk-Potoczna K, Lorkiewicz-Muszyńska D, et al. Introducing a simple method of maxillary sinus volume assessment based on linear dimensions. *Ann Anat* 2018; **215**: 47–51. doi: https://doi.org/10.1016/j.aanat.2017.09.010
16. Sahlstrand-Johnson P, Jannert M, Strömbeck A, Abul-Kasim K. Computed tomography measurements of different dimensions of maxillary and frontal sinuses. *BMC Med Imaging* 2011; **11**: 8. doi: https://doi.org/10.1186/1471-2342-11-8
17. Duerinckx AJ, Hall TR, Whyte AM, Lufkin R, Kangarloo H. Paranasal sinuses in pediatric patients by MRI: normal development and preliminary findings in disease. *Eur J Radiol* 1991; **13**: 107–12. doi: https://doi.org/10.1016/0720-048X(91)90090-I
18. Adibelli ZH, Songu M, Adibelli H. Paranasal sinus development in children: a magnetic resonance imaging analysis. *Am J Rhinol Allergy* 2011; **25**: 30–5. doi: https://doi.org/10.2500/ajra.2011.25.3552
19. Giacomini G, Pavan ALM, Altemani JMC, Duarte SB, Fortaleza CMCB, Miranda JRdeA, et al. Computed tomography-based volumetric tool for standardized measurement of the maxillary sinus. *PLoS One* 2018; **13**: e0190770. doi: https://doi.org/10.1371/journal.pone.0190770
20. Whyte A, Chapeikin G. Opaque maxillary antrum: a pictorial review. *Australas Radiol* 2005; **49**: 203–13. doi: https://doi.org/10.1111/j.1440-1673.2005.01432.x
21. Erdem T, Aktas D, Erdem G, Miman MC, Ozturan O, hypoplasia Msinus. Maxillary sinus hypoplasia.. *Rhinology* 2002; **40**: 150–3.
22. de Dorlodot C, Collet S, Rombaux P, Horoi M, Hassid S, Eloy P. Chronic maxillary atelectasis and silent sinus syndrome: two faces of the same clinical entity. *Eur Arch Otorhinolaryngol* 2017; **274**: 3367–73. doi: https://doi.org/10.1007/s00405-017-4622-8
23. Illner A, Davidson HC, Harnsberger HR, Hoffman J. The silent sinus syndrome: clinical and radiographic findings. *AJR Am J Roentgenol* 2002; **178**: 503–6. doi: https://doi.org/10.2214/ajr.178.2.1780503
24. Kim HY, Kim M-B, Dhong H-J, Jung YG, Min J-Y, Chung S-K, et al. Changes of maxillary sinus volume and bony thickness of the paranasal sinuses in longstanding pediatric chronic rhinosinusitis. *Int J Pediatr Otorhinolaryngol* 2008; **72**: 103–8. doi: https://doi.org/10.1016/j.ijporl.2007.09.018
25. Kim HJ, Friedman EM, Sulek M, Duncan NO, McCluggage C. Paranasal sinus development in chronic sinusitis, cystic fibrosis, and normal comparison population: a computerized tomography correlation study. *Am J Rhinol* 1997; **11**: 275–81. doi: https://doi.org/10.2500/105065897781446676
26. Price DL, Friedman O. Facial asymmetry in maxillary sinus hypoplasia. *Int J Pediatr Otorhinolaryngol* 2007; **71**: 1627–30. doi: https://doi.org/10.1016/j.ijporl.2007.06.014
27. Ozcan KM, Hizli O, Ulusoy H, Coskun ZU, Yildirim G. Localization of orbit in patients with maxillary sinus hypoplasia: a radiological study. *Surgical and Radiologic Anatomy* 2018; **40**: 1099–104. doi: https://doi.org/10.1007/s00276-018-2054-9
28. Song SY, Hong JW, Roh TS, Kim YO, Kim DW, Park BY. Volume and distances of the maxillary sinus in craniofacial deformities with midfacial hypoplasia. *Otolaryngol Head Neck Surg* 2009; **141**: 614–20. doi: https://doi.org/10.1016/j.otohns.2009.08.018
29. Woodworth BA, Ahn C, Flume PA, Schlosser RJ. The delta F508 mutation in cystic fibrosis and impact on sinus development. *Am J Rhinol* 2007; **21**: 122–7. doi: https://doi.org/10.2500/ajr.2007.21.2905
30. Kim S-H, Kim K-H, Seo B-M, Koo K-T, Kim T-I, Seol Y-J, et al. Alveolar bone regeneration by transplantation of periodontal ligament stem cells and bone marrow stem cells in a canine peri-implant defect model: a pilot study. *J Periodontol* 2009; **80**: 1815–23. doi: https://doi.org/10.1902/jop.2009.090249
31. Kalyvas D, Kapsalas A, Paikou S, Tsiklakis K. Thickness of the Schneiderian membrane and its correlation with anatomical structures and demographic parameters using CBCT tomography: a retrospective study. *International Journal of Implant Dentistry* 2018; **4**: 32. doi: https://doi.org/10.1186/s40729-018-0143-5
32. Drumond J, Allegro B, Novo N, de Miranda S, Sendyk W. Evaluation of the prevalence of maxillary sinuses abnormalities through spiral computed tomography (CT. *Int Arch Otorhinolaryngol* 2017; **21**: 126–33. doi: https://doi.org/10.1055/s-0036-1593834
33. Scarfe WC, Langlais RP, Ohba T, Kawamata A, Maselle I. Panoramic radiographic patterns of the infraorbital canal and anterior superior dental plexus. *Dentomaxillofac Radiol* 1998; **27**: 85–92. doi: https://doi.org/10.1038/sj.dmfr.4600326
34. Nguyen DC, Farber SJ, Um GT, Skolnick GB, Woo AS, Patel KB, Patel P. Anatomical study of the Intraosseous pathway of the infraorbital nerve. *Journal of Craniofacial Surgery* 2016; **27**: 1094–7. doi: https://doi.org/10.1097/SCS.0000000000002619
35. Lantos JE, Pearlman AN, Gupta A, Chazen JL, Zimmerman RD, Shatzkes DR, et al. Protrusion of the infraorbital nerve into the maxillary sinus on CT: prevalence, proposed grading method, and suggested clinical implications. *AJNR Am J Neuroradiol* 2016; **37**: 349–53. doi: https://doi.org/10.3174/ajnr.A4588

36. Yura S, Kato T, Ooi K, Izumiyama Y. Access to the maxillary sinus using a bone flap with sinus mucosal and mucoperiosteal pedicles. *Oral Surgery, Oral Medicine, Oral Pathology, Oral Radiology, and Endodontology* 2010; **109**: e8–12. doi: https://doi.org/10.1016/j.tripleo.2009.09.012
37. Rapani M, Rapani C, Ricci L. Schneider membrane thickness classification evaluated by cone-beam computed tomography and its importance in the predictability of perforation. retrospective analysis of 200 patients. *British Journal of Oral and Maxillofacial Surgery* 2016; **54**: 1106–10. doi: https://doi.org/10.1016/j.bjoms.2016.08.003
38. Lin Y-H, Yang Y-C, Wen S-C, Wang H-L. The influence of sinus membrane thickness upon membrane perforation during lateral window sinus augmentation. *Clin. Oral Impl. Res* 2015; **00**: 1–6.
39. Boeddinghaus R, Whyte A. *Trends in maxillofacial imaging Clin Radiol* 2018; **73**: 4–18.
40. Tian X-mei, Qian L, Xin X-zhen, Wei B, Gong Y. An analysis of the proximity of maxillary posterior teeth to the maxillary sinus using cone-beam computed tomography. *J Endod* 2016; **42**: 371–7. doi: https://doi.org/10.1016/j.joen.2015.10.017
41. Sánchez-Pérez A, Boracchia AC, López-Jornet P, Boix-García P. Characterization of the maxillary sinus using cone beam computed tomography. A retrospective radiographic study. *Implant Dent* 2016; **25**: 762–9. doi: https://doi.org/10.1097/ID.0000000000000485
42. Schriber M, von Arx T, Sendi P, Jacobs R, Suter V, Bornstein M. Evaluating maxillary sinus septa using cone beam computed tomography: is there a difference in frequency and type between the dentate and edentulous posterior maxilla? *Int J Oral Maxillofac Implants* 2017; **32**: 1324–32. doi: https://doi.org/10.11607/jomi.5854
43. Cavalcanti MC, Guirado TE, Sapata VM, Costa C, Pannuti CM, Jung RE, et al. Maxillary sinus floor pneumatization and alveolar ridge resorption after tooth loss: a cross-sectional study. *Braz Oral Res*. 2018; **32**vol32.00642018; 32: e64.. doi: https://doi.org/10.1590/1807-3107bor-2018.vol32.0064
44. Chan H-L, Wang H-L. Sinus pathology and anatomy in relation to complications in lateral window sinus augmentation. *Implant Dent* 2011; **20**: 406–12. doi: https://doi.org/10.1097/ID.0b013e3182341f79
45. Sharan A, Madjar D. Correlation between maxillary sinus floor topography and related root position of posterior teeth using panoramic and cross-sectional computed tomography imaging. *Oral Surgery, Oral Medicine, Oral Pathology, Oral Radiology, and Endodontology* 2006; **102**: 375–81. doi: https://doi.org/10.1016/j.tripleo.2005.09.031
46. Chan H-L, Suarez F, Monje A, Benavides E, Wang H-L. Evaluation of maxillary sinus width on cone-beam computed tomography for sinus augmentation and new sinus classification based on sinus width. *Clin Oral Implants Res* 2014; **25**: 647–52. doi: https://doi.org/10.1111/clr.12055
47. Bornstein MM, Horner K, Jacobs R. Use of cone beam computed tomography in implant dentistry: current concepts, indications and limitations for clinical practice and research. *Periodontology* 2017; **2000**: 51–72.
48. Pauwels R, Jacobs R, Singer SR, Mupparapu M. CBCT-based bone quality assessment: are Hounsfield units applicable? *Dentomaxillofac Radiol* 2015; **44**: 20140238. doi: https://doi.org/10.1259/dmfr.20140238
49. Lopes LJ, Gamba TO, Bertinato JVJ, Freitas DQ. Comparison of panoramic radiography and CBCT to identify maxillary posterior roots invading the maxillary sinus. *Dentomaxillofac Radiol* 2016; **45**: 20160043.. doi: https://doi.org/10.1259/dmfr.20160043
50. Kirkham-Ali K, La M, Sher J, Sholapurkar A. Comparison of cone-beam computed tomography and panoramic imaging in assessing the relationship between posterior maxillary tooth roots and the maxillary sinus: a systematic review. *J Investig Clin Dent* 2019; **28**: e12402: e12402: .
51. Kilic C, Kamburoglu K, Yuksel SP, Ozen T. An assessment of the relationship between the maxillary posterior teeth root tips using dental cone-beam computerized tomography. *Eur J Dent* 2010; **4**: 462–7.
52. Kang SH, Kim BS, Kim Y. Proximity of posterior teeth to the maxillary sinus and buccal bone thickness: a biometric assessment using cone-beam computed tomography. *J Endod* 2015; **41**: 1839–46. doi: https://doi.org/10.1016/j.joen.2015.08.011
53. Daines SM, Orlandi RR. Chronic rhinosinusitis. *Facial Plast Surg Clin North Am* 2012; **20**: 1–10. doi: https://doi.org/10.1016/j.fsc.2011.10.001
54. Vaid S, Vaid N. Normal anatomy and anatomic variants of the paranasal sinuses on computed tomography. *Neuroimaging Clin N Am* 2015; **25**: 527–48. doi: https://doi.org/10.1016/j.nic.2015.07.002
55. Beale TJ, Madani G, Morley SJ. Imaging of the paranasal sinuses and nasal cavity: normal anatomy and clinically relevant anatomical variants. *Seminars in Ultrasound, CT and MRI* 2009; **30**: 2–16. doi: https://doi.org/10.1053/j.sult.2008.10.011
56. Vaid S, Vaid N, Rawat S, Ahuja AT. An imaging checklist for pre-FESS CT: framing a surgically relevant report. *Clin Radiol* 2011; **66**: 459–70. doi: https://doi.org/10.1016/j.crad.2010.11.010
57. Prasanna LC, Mamatha H. The location of maxillary sinus Ostium and its clinical application. *Indian J Otolaryngol Head Neck Surg* 2010; **62**: 335–7. doi: https://doi.org/10.1007/s12070-010-0047-z
58. Rodella LF, Buffoli B, Labanca M, Rezzani R. A review of the mandibular and maxillary nerve supplies and their clinical relevance. *Arch Oral Biol* 2012; **57**: 323–34. doi: https://doi.org/10.1016/j.archoralbio.2011.09.007
59. Rosano G, Taschieri S, Gaudy J-F, Weinstein T, Del Fabbro M. Maxillary sinus vascular anatomy and its relation to sinus lift surgery. *Clin Oral Implants Res* 2011; **22**: 711–5. doi: https://doi.org/10.1111/j.1600-0501.2010.02045.x
60. Varela-Centelles P, Loira-Gago M, Seoane-Romero JM, Takkouche B, Monteiro L, Seoane J. Detection of the posterior superior alveolar artery in the lateral sinus wall using computed tomography/cone beam computed tomography: a prevalence meta-analysis study and systematic review. *Int J Oral Maxillofac Surg* 2015; **44**: 1405–10. doi: https://doi.org/10.1016/j.ijom.2015.07.001
61. Rysz M, Ciszek B, Rogowska M, Krajewski R. Arteries of the anterior wall of the maxilla in sinus lift surgery. *Int J Oral Maxillofac Surg* 2014; **43**: 1127–30. doi: https://doi.org/10.1016/j.ijom.2014.02.018